

Upgrade of the CMS Tracker for the High Luminosity LHC

Marko Dragicevic^{*†}

Institute of High Energy Physics, Vienna

E-mail: marko.dragicevic@oeaw.ac.at

A significant upgrade of the LHC accelerator is planned to become operational mid of the next decade. This High Luminosity LHC will increase the design luminosity by a factor of five to about $5 \times 10^{34} \text{ cm}^{-2}\text{s}^{-1}$ or even beyond, making an upgrade of the detectors unavoidable. To cope with this environment, the outer tracker of the CMS experiment has to face an increase in particle density inducing more radiation damage and higher occupancy. Furthermore, the tracker has to provide information to the level one hardware trigger.

The CMS Tracker Collaboration has developed a concept for a new tracking system, which uses intelligent dual sensor modules with high granularity. We will describe the main constituents of this new tracking detector concept.

24th International Workshop on Vertex Detector - VERTEX2015-

1-5 June 2015

Santa Fe, New Mexico, USA

^{*}Speaker.

[†]On behalf of the CMS Tracker Collaboration

1. Introduction

The Large Hadron Collider LHC was designed to deliver about 300 fb^{-1} during its 10 year lifetime. Continuing the operation of the accelerator at its design luminosity of $10^{34} \text{ cm}^{-2}\text{s}^{-1}$ would only marginally increase the physics outcome. To increase the amount of statistics collected within a certain timeframe, the accelerator needs to be operated at a significantly higher luminosity. It is planned to upgrade the LHC accelerator and crucial parts of the pre-accelerator complex at CERN to be able to operate at about five times the original design luminosity in the next decade. This High Luminosity LHC (HL-LHC) would achieve a luminosity of $5 \times 10^{34} \text{ cm}^{-2}\text{s}^{-1}$. A more detailed discussion on the physics potential of the HL-LHC can be found in [1].

To cope with the increase in radiation damage and a pile-up of up to 140, several subdetectors have to be replaced or partially upgraded. In particular the tracking system will have reached its end of lifetime due to radiation damage by then and the new challenges will require a significantly different and more powerful design. The CMS Tracker collaboration has proposed an upgrade to the existing detector, which is described in more detail in a technical proposal [2].

The challenges the new tracker has to face are threefold:

1. Higher density of tracks which requires an increase in granularity of the detector elements.
2. Increase in radiation which requires more radiation hard components and sensors in particular.
3. Information has to be passed to the level 1 trigger system at every bunch crossing which requires data selection inside the active volume.

2. Radiation Hard Silicon Sensors

To investigate the suitability of currently available silicon sensor materials for the operation in an HL-LHC environment, the CMS Tracker collaboration has started an extensive irradiation and measurement campaign as reported for example in [3] and [4]. More than 30 different structures, from strip and pixel sensors to dedicated test structures, have been designed and manufactured at a single producer¹ to ensure comparability among the different materials and processes used. The structures have been produced on four different wafer materials: Float Zone (FZ), deep diffused Float Zone (ddFZ), magnetic Czochalski (mCZ) and epitaxial silicon (Epi). The physical and active thicknesses varied between $50 \mu\text{m}$ to $320 \mu\text{m}$. Furthermore, all materials were ordered in n- and p-type and strip isolation for the n-on-p process was ensured using p-stop or p-spray techniques. Finally a few wafers were also produced with a second metalisation to test different on-sensor routing patterns. Table 2 summarises the received number of wafers per material.

The structures from the different materials were irradiated with neutrons and protons at different energies from different sources: 23 MeV protons from the compact cyclotron at KIT², 800 MeV protons from the LINAC at LANSCE³, 23 GeV protons from PS at CERN⁴ and neutrons from the

¹Hamamatsu Photonics K.K. (HPK)

²http://www.ekp.kit.edu/english/irradiation_center.php

³<http://lansce.lanl.gov/about/linac.shtml>

⁴<https://irradiation.web.cern.ch/irradiation/irrad1.htm>

Material and active thickness	n-on-p	p-on-n (p-stop)	p-on-n (p-spray)
FZ 320 μm	6/6	6/6	6/6
ddFZ 200 μm (deep diffusion)	6/6	6/6	6/6
FZ 200 μm (wafer thinning)	6/6	6/0	4/0
FZ 200 μm (with 2nd metal layer)	6/6	6/6	6/6
FZ 120 μm (deep diffusion)	6/6	6/6	6/6
FZ 120 μm (on carrier wafer)	6/0	6/0	4/0
MCz 200 μm	6/6	6/6	6/6
Epi 100 μm	2/6	6/6	6/6
Epi 70 μm	0/4	0/0	0/0
Epi 50 μm	6/6	6/6	6/6

Table 1: Wafer materials, thicknesses and production processes which were studied for the CMS tracker upgrade. The numbers indicate the number of wafers ordered/delivered. The Epi 100 μm material could not be delivered in the quantity that was originally ordered due to yield problems at the manufacturer. The missing wafers were substituted by Epi 70 μm .

TRIGA Mark II nuclear reactor at JSI⁵ [5]. Particle fluences were chosen to correspond to those expected in the tracker after 3000 fb^{-1} at certain radii as described in table 2.

radius	protons Φ_{eq} [cm^{-2}]	neutrons Φ_{eq} [cm^{-2}]	total Φ_{eq} [cm^{-2}]
60 cm	3×10^{14}	4×10^{14}	7×10^{14}
20 cm	1×10^{15}	5×10^{14}	1.5×10^{15}
15 cm	1.5×10^{15}	6×10^{14}	2.1×10^{15}
10 cm	3×10^{15}	7×10^{14}	3.7×10^{15}
5 cm	1.3×10^{16}	1×10^{15}	1.4×10^{16}

Table 2: Proton, neutron and combined fluences after an integrated luminosity of 3000 fb^{-1} at certain radii in the tracker.

2.1 Results

Our measurements confirmed that thick n-type sensors show a more pronounced signal degradation with irradiation than p-type sensors as shown in figure 1 (left) and as previously reported for example in [6]. The charge collected in thin sensors with a thickness of 200 μm matches those of thick sensors beyond a fluence of $10^{15} \text{neqcm}^{-2}$ as shown in figure 1 (right). Furthermore, we have observed very high charges collected in n-type sensors after fluences beyond $10^{14} \text{neqcm}^{-2}$. These charges cannot originate from the incident particle but are caused by micro-discharges at the strip edges that intensify with increasing accumulation of oxide charge as shown in simulations reported in [7]. This effect creates an increase in non-Gaussian noise and ultimately causes signals with enough charge to be detected as random ghost hits.

⁵<http://www.rcp.ijs.si/ric/description-a.html>

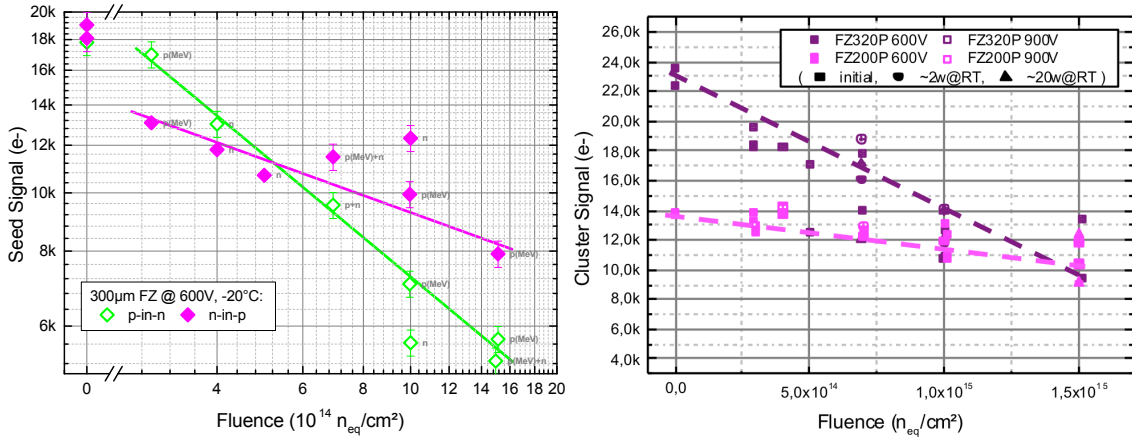


Figure 1: Charge collected on the seed strip (strip with the highest signal in a cluster) vs. fluence for 600 V biasing at -20°C after short annealing (50 h to 250 h) at room temperature, for a sensor thickness of 320 μm (left). Charge collected per cluster vs. fluence for 600 V and 900 V and for 200 μm and 300 μm of active thickness (right). Lines are drawn to guide the eye.

For mCZ materials we have observed no loss of signal after annealing as shown in figure 2. The full depletion voltage of FZ materials changes significantly with annealing. After more than 20 weeks of annealing at room temperature they are not fully depleted at 600 V while for mCZ the full depletion voltage stays constant and they operate fully depleted at that voltage. The charges lost in the undepleted regions of the FZ sensors can be recovered by increasing the depletion voltage to 900 V.

2.2 Summary

Following the results presented above we have selected p-type materials as baseline for the upgrade. They show less signal degradation with fluence and we did not observe random ghost hits even at the highest fluences. An active sensor thickness of 200 μm is preferred since they produce smaller dark current while delivering a similar signal after about $10^{15} n_{eq} \text{cm}^{-2}$. The mCZ materials show advantages over FZ in their annealing behaviour.

3. Detector Modules

The capability to select and reduce data before sending it to the level 1 trigger system at every bunch crossing is incorporated into the design of the modules. The general idea, as shown in figure 3 (left), is to estimate the incident angle of particles by measuring the displacement of the track on two closely spaced sensors. The incident angle at a given radius from the interaction point gives a good indication of the transverse momentum of a charged particle in a magnetic field.

The incident angle is then measured by a module which consists of two sensors that are separated by a few millimeters. The displacement of the track from the sensor that is nearer to the interaction point to the one that is farther away gives a good estimate on the angle. An acceptance window can be defined, where stubs which are within the window originate from particles with

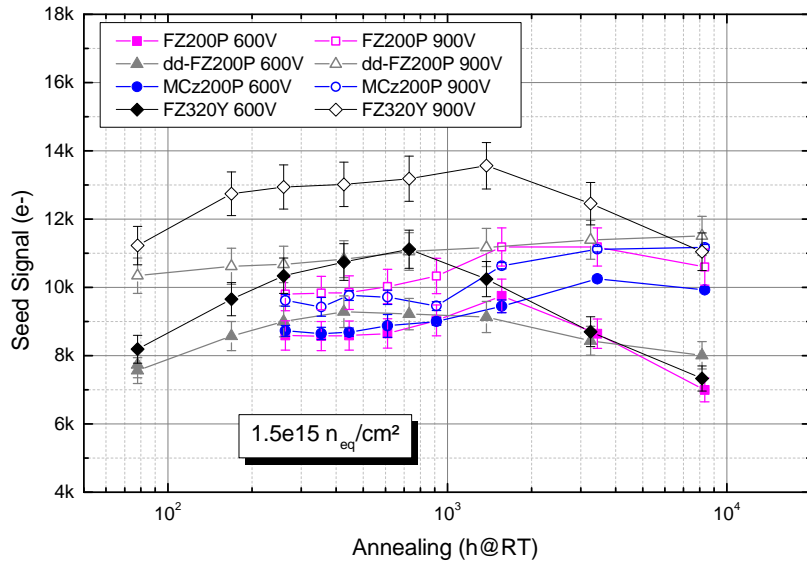


Figure 2: Seed signal as a function of annealing. The annealing was performed at 60° C or 80° C and the scaling to 21° C was done according to the annealing behaviour of the leakage current. FZ320Y is 320 μm thick p-type FZ with p-spray strip isolation.

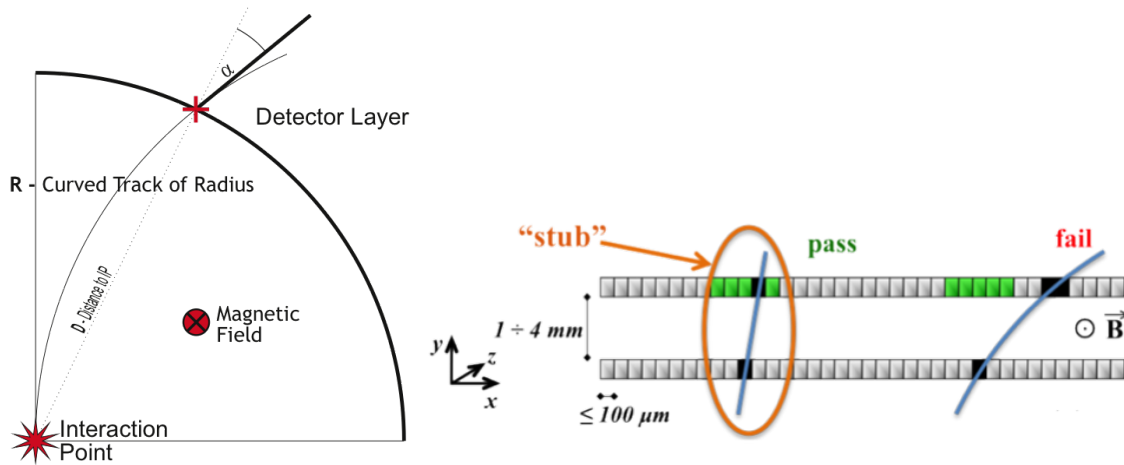


Figure 3: The incident angle of a charged particle in a given magnetic field and on a sensor at a given distance from the interaction point depends on the curvature of the track which is determined by its transverse momentum (left). The incident angle can be estimated by combining the measurements of two closely spaced sensors and determining the displacement (right).

stiff tracks and therefore a transverse momentum exceeding the threshold. Only the information associated with these hits is sent to the trigger, while information for tracks below the momentum threshold is stored on the module. Only if the level 1 trigger accepts the event, the readout of the full information is initiated.

This module concept has already been successfully demonstrated in a beam test at DESY [8]

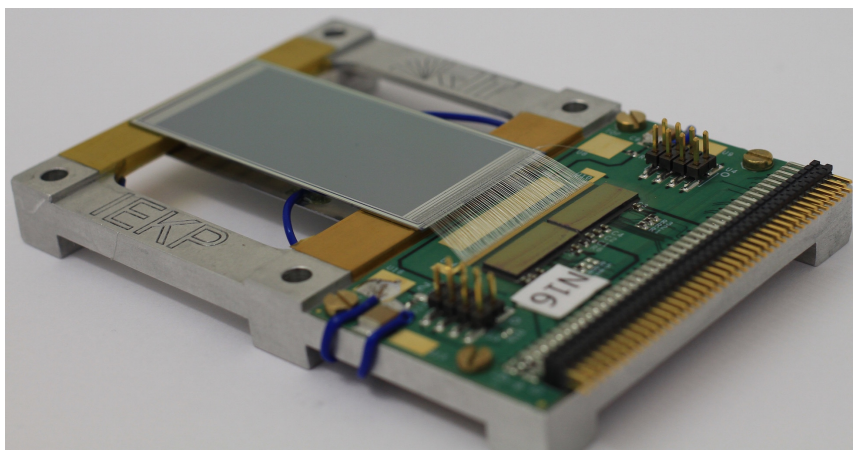


Figure 4: Mini module with two closely spaced strip sensors and two CBC2 readout chips.

using a mini module as shown in figure 4. The concept has been advanced into two different module designs, the 2S module for the outer and the PS module for the inner layers of the tracker.

3.1 The 2S Module

The 2S module⁶ is built around two AC-coupled strip sensors of approximately $10 \times 10 \text{ cm}^2$ size. The pitch of the strips is $90 \mu\text{m}$ and each strip is segmented into two 5 cm long ones resulting in 2×2016 strips which can be read out from both ends of the sensor. The readout is done by 8 CBC (CMS Binary Chip) chips on each end, where each chip reads strips from the top and bottom sensor alternately. The CIC (Concentrator ASIC) collects data from 8 CBCs, reformats and compresses the information and passes it to the LP-GBT (Low Power GigaBit Transceiver). Power is provided to the module by a two stage DC-DC converter. The chips are bump bonded to the hybrids while the connection to the sensors is made by conventional, low cost wire bonding. The connection pads for the bottom sensor are provided by bending of the flexible hybrid around its support. The module is reinforced by carbon fiber stiffeners and spacers made from parylene coated Al-CF composites. A representation of the module design is shown in figure 5.

3.2 The PS Module

The PS module⁷ uses a DC-coupled pixel and a AC-coupled strip sensor of approximately $5 \times 10 \text{ cm}^2$ size. The pitch of the strip sensors is identical to the column pitch of the pixel sensor at $100 \mu\text{m}$. The strips are segmented into two parts, similar to the 2S sensors, while in the pixel sensor each pixel has a length of 1.5 mm resulting in 32 pixels per column. Since the pixels are comparably large we like to refer to them as macro-pixels. The PS module shares some electronic components with the 2S module like CIC, LP-GBT and similar DC-DC converters. This ensures that the back-end readout communicates with PS and 2S modules in the same way. The mechanical components are based on the same materials as well, with exception of the Carbon Fiber Reinforced

⁶The name 2S indicates that the module uses 2 Strip sensors

⁷The name PS indicates that the module uses a Pixel and a Strip sensor

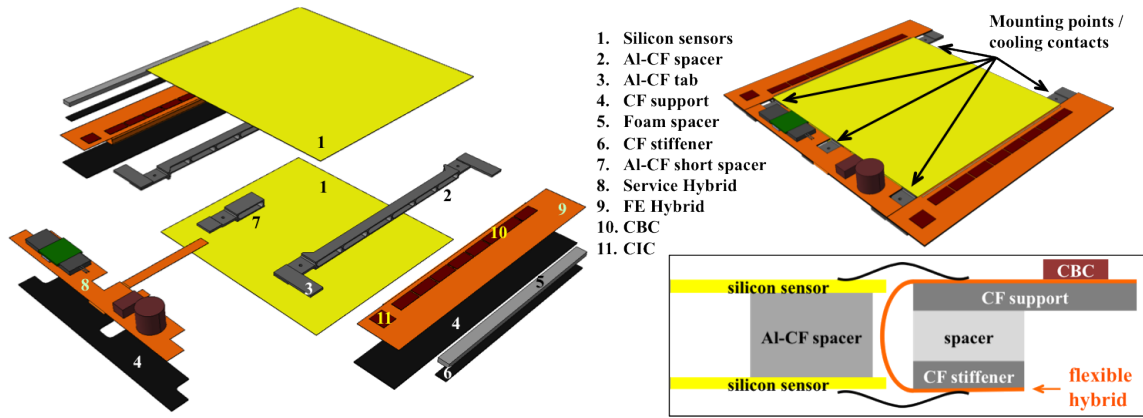


Figure 5: Exploded view of the 2S module components (left), 3D view of the assembled module (upper right), and a sketch of the FE Hybrid folded around its support (lower right). The module is mounted on five cooling elements on the mechanical support structure.

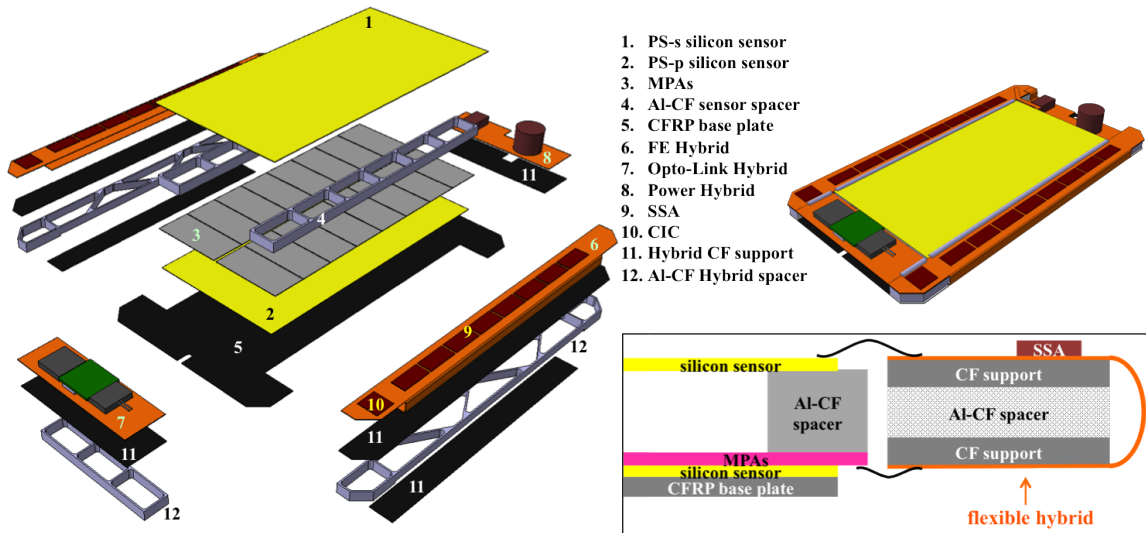


Figure 6: Exploded view of the PS module components (left), 3D view of the assembled module (upper right), and a sketch of the FE Hybrid folded around its support (lower right). The base plate is glued onto a flat surface on the support structure that is kept cold during operation.

Polymer (CFRP) base plate. The main differences are in the sensors and subsequently the front-end readout chips. The macro-pixel sensor requires a pixel-like readout concept where the chips cover the full surface of the sensor and are bump bonded to it. To read out the full sensor 16 of these so-called Macro Pixel ASICs (MPA) are needed. The signals from the top strip sensors are acquired by the Short Strip ASIC (SSA) which sends the data to the MPA. The stub finding logic is implemented in the MPA as well. Eight of the SSAs are connected to each end of the sensor using wire bonds from the sensor to the hybrid and bump bonds from the hybrid to the chips. A representation of the module design is shown in figure 6.

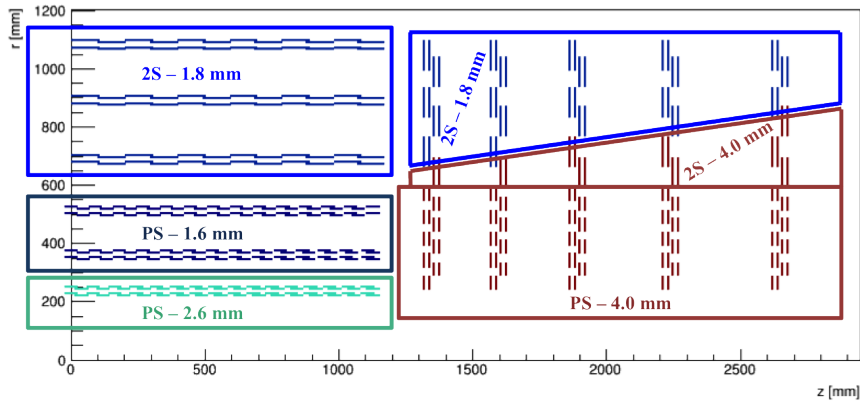


Figure 7: Basic layout of the tracker. The sensor spacing is optimized to obtain a p_T threshold of 2 GeV for the stub selection in all module locations.

4. The Tracker Layout

The layout of the new tracking system follows a standard barrel and endcap geometry as shown in figure 7. PS modules are used at radii below 60 cm where a higher granularity is needed, while the cheaper and less power consuming 2S modules are placed at radii larger than 60 cm. The spacing of the sensors on PS and 2S modules (PS: 1.6 mm, 2.6 mm and 4 mm, 2S: 1.8 mm and 4 mm) is optimised depending on their location. Nevertheless, only two basic module types are sufficient to equip the full detector. The proposed geometry gives a similar number of hits per track compared to the existing tracker but at a larger η coverage⁸ as shown in figure 8 (left). The amount of material is significantly reduced compared to the existing tracker as shown in 8 (right).

5. Summary and Outlook

The CMS Tracker collaboration proposes a mature concept for a new tracking system for operation of the CMS Detector at HL-LHC condition. Most of the main concepts have been demonstrated while the final specifications will be defined throughout 2016. Prototyping for most of the key components has already started in 2015. The publication of the technical design report is planned for the beginning of 2017.

References

- [1] F. Gianotti *et al.*, **Physics potential and experimental challenges of the LHC luminosity upgrade.** *European Physical Journal*, C39:293–333, 2005.
- [2] The CMS Collaboration, **Technical Proposal for the Phase-II Upgrade of the CMS Detector.** *CERN-LHCC-2015-010*, 2015.
- [3] K.-H. Hoffmann, **Campaign to identify the future CMS tracker baseline.** *Nuclear Instruments and Methods A*, 658, 30-35, 2011.

⁸The proposed geometry includes a very forward extension of the pixel detector which increases the coverage up to $\eta = 4$.

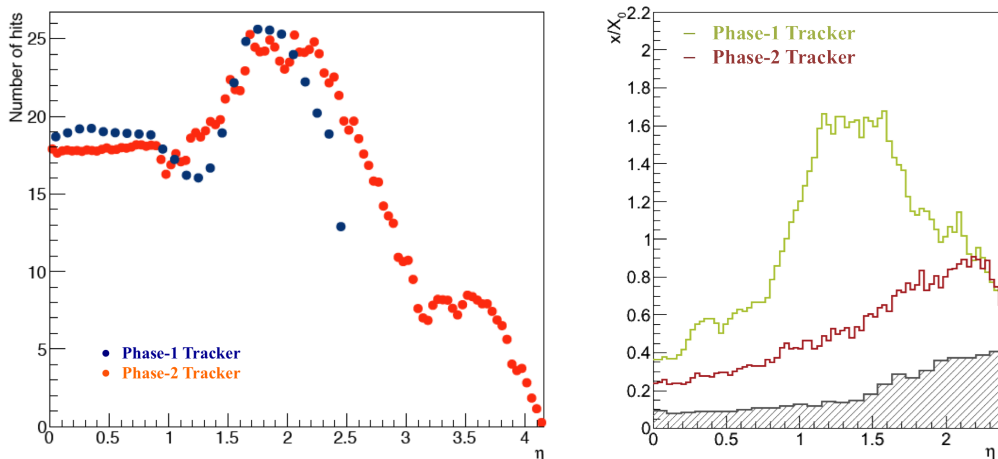


Figure 8: Number of hits (left) and radiation length (right) versus η for the new tracker and the existing tracker after the phase 1 upgrade of the pixel detector. The Phase-2 Tracker includes a very forward pixel extension. The radiation length distribution is shown for the tracking acceptance of the same phase 1 tracker, and reflects only the material inside the tracking volume; the expected contribution of the phase 1 pixel detector (hashed histogram) is provisionally used also for the new tracker.

- [4] A. Dierlamm, **Characterisation of silicon sensor materials and designs for the CMS Tracker Upgrade.**
Proceedings of Science, PoS(VERTEX 2012) 016, 2012.
- [5] L. Snoj, G. Žerovnik, and A. Trkov, **Computational analysis of irradiation facilities at the JSI TRIGA reactor.**
Applied Radiation and Isotopes 70, 483-488, 2012.
- [6] G.-L. Casse, A. Affolder, P.P. Allport and M. Wormald, **Measurements of charge collection efficiency with microstrip detectors made on various substrates after irradiations with neutrons and protons with different energies.**
Proceedings of Science, PoS(VERTEX 2008) 036, 2008.
- [7] R. Dalal, A. Bhardwaj, K. Ranjan, M. Moll and A. Elliott-Peisert, **Combined effect of bulk and surface damage on strip insulation properties of proton irradiated n+-p silicon strip sensors.**
Journal of Instrumentation, Volume 9, 2014.
- [8] D. Braga et al., **Beam test performance of the 2S prototype module for the High Luminosity Upgrade of the CMS Strip Tracker.**
3rd Workshop on Intelligent Trackers, WIT 2014, 14-16 May 2014, to be published on JINST.